Journal of Applied Polymer Science

Novel polyketones with pendant imidazolium groups as nanodispersants of hydrophobic antibiotics

Esteban Araya-Hermosilla,[1,2] Sandra L. Orellana,[1] Claudio Toncelli,[2] Francesco Picchioni,[2] Ignacio Moreno-Villoslada[1]

[1]Instituto de Ciencias Químicas, Facultad de Ciencias, Universidad Austral de Chile, Casilla 567, Valdivia, Chile

[2]Department of Chemical Engineering/Product technology, University of Groningen, Nijenborgh 4, 9747AG, Groningen, The Netherlands

Correspondence to: I. Moreno-Villoslada (E-mail: imorenovilloslada@uach.cl)

ABSTRACT: In this work, we present a new method to nanodisperse the pH-sensitive antibiotics oxolinic acid and flumequine by the use of a pH-sensitive synthetic polyketone derivative with amphiphilic characteristics. The pH-sensitive polymer bears imidazolium residues on pendant groups as weak acids, and its solvophobic properties can be tuned by changing the pH. While the antibiotics are soluble in water at pHs higher than 7.0 for flumequine and 8.4 for oxolinic acid, and the polymer is soluble in water at pHs lower than 5.5, nanoprecipitates presenting hydrodynamic radius of 35–100 nm and positive zeta potential containing both the polymer and any of the antibiotics are formed at pH 6.8 by mixing stock solutions whose pH has been adjusted to 5.4 for the polymer and higher than 10 for the antibiotics. The out-of-equilibrium process occurring upon mixing both solutions produces pH changing, molecular arrangement, and a controlled collapse of the system in the form of nano- and submicron particles. The driving forces for the arrangements are found among hydrophobic forces, long-range electrostatic interactions, and short range aromatic–aromatic interactions. © 2015 Wiley Periodicals, Inc. J. Appl. Polym. Sci. **2015**, *132*, 42363.

KEYWORDS: functionalization of polymers; nanostructured polymers; polyelectrolytes

Received 29 January 2015; accepted 11 April 2015

DOI: 10.1002/app.42363

INTRODUCTION

Amphiphilic polymers[1,2] can form several structures in the nano- and micrometric range, such as unimolecular micelles or multimolecular aggregates.[3,4] Tunable amphiphilic polymers represent a new class of materials for practical applications. By tuning the amphiphilic behavior of polymers, stimuli responsive materials may be obtained. As a matter of example, poly(*N*-isopropylacrylamide) is recognized by its temperature-sensitive solvophobic properties.[5] The collapse of water-soluble polymers and consequent precipitation is an out-of-equilibrium process[6–8] that may be produced as a response to changes on environmental conditions that modifies the hydrophilic properties of the polymers.[9–11] Changes on the pH of a solution can result in the collapse of weak polyelectrolytes undergoing acid–base equilibrium.[12–16] Copolymers based on acrylic acid and methyl methacrylate have been tested as coatings of pharmaceutical products for oral administration due to their pH-sensitive properties.[17] Polychelatogens may undergo phase separation when their binding sites become saturated with metal ions.[18]. The amphiphilic characteristics of polyelectrolytes may be also tuned if ion pairs or hydrophobic complexes are formed with organic counterions.[19–21] These charged organic counterions may induce the collapse of polymeric systems when they undergo secondary interactions such as short-range electrostatic interactions, hydrogen bonding, or aromatic–aromatic interactions.[22–25] The aggregation of polyelectrolyte chains by means of these secondary interactions may result in structures with defined features, such as shape, size, and zeta potential.[24–26] Controlled changes in solution properties may allow tuning some of these characteristics, and can lead to a controlled polymer collapse. The same principles may be applied to other out-of-equilibrium processes such as the formation of polyelectrolyte deposits upon solvent evaporation.

Polyketones represent an interesting class of polymeric materials.[27] Perfectly alternating copolymers of carbon monoxide and unsaturated hydrocarbon monomers (such as propylene and ethylene) can be easily obtained using palladium derivatives as catalysts. The resulting polymers bear 1,4-dicarbonyl moieties that may, in a second step, be easily functionalized by reaction with a primary amine through the Paal-Knorr modification. Upon this reaction, 1,4-dicarbonyl groups in the polyketones are transformed into *N*-substituted pyrrole groups.[23,28] The pyrrole groups become part of the main chain, providing rigidity and

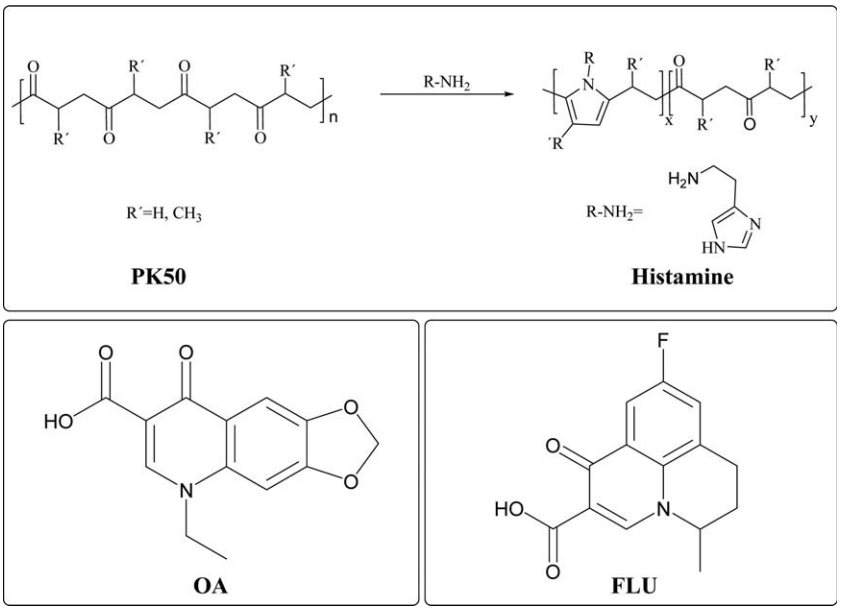

Figure 1. Paal-Knorr reaction of PK50 with histamine, and structures of OA and FLU.

hydrophobicity, whereas different functional groups may be incorporated in the pendant groups by using different primary amines, thus providing different functionalities and physicochemical properties. This reaction is a solvent-free one-pot reaction, which allows fine tailoring of the polymer properties, and yields water as the sole by-product. Alternated (ethene/propene)/CO polyketones have been recently functionalized with primary amines containing charged aromatic groups, such as histamine, to give rise to a polyketone with imidazolium pendant groups (PK-Im).[23] An excess of this aromatic cationic polymer has been proved to bind and disperse an aromatic, anionic water-soluble dye such as 5,10,15,20-tetrakis-(4-sulfonatophenyl)-porphyrin whereas aliphatic, cationic polymers induce the dye self-aggregation, indicating the role of hydrophobic and aromatic–aromatic interactions on the binding properties observed.[23]

The formation of nanostructures that contain target molecules is interesting for many purposes. Nanoformulated antibiotics represent an advantage for more secure pharmaceutical applications, having implications in bioavailability, distribution, and efficacy. Some antibiotics present charged aromatic groups, so that they are prone to undergo aromatic–aromatic interactions. In particular, quinolones are broad-spectra bactericidal compounds, for which adequate vehiculization would result in improved environmental and biological security. Their antibacterial mechanism is based on the inhibition of DNA-gyrase, which renders an unstable condensation and configuration of the bacterial DNA during the cell division process.[29] The quinolones oxolinic acid (OA) and flumequine (FLU), are commonly used in aquaculture as prophylactics to prevent diseases or as chemotherapeutic agents to control diseases. OA and FLU present a low bioavailability to aquatic animals, which may result in high concentration of antibiotic residues in aquatic environments.[30] Their overuse produces bacterial resistance, prevalence of diseases,[31] and risks to human health. Both antibiotics are relatively insoluble in water. Developing methods to encapsulate OA and FLU could find an application to improve both animal and human health treatments, with minimal environmental impact. Nanoformulated antibiotics may be included in pellets to feed fishes, with the aim of providing improved performances such as minimizing loss of drug in the feces, decreasing the

Table I. Final pH and Component Concentration of the Formulations Containing OA and PK-Im

OA/PK-Im	[PK-Im] × 10^4 (M)	[OA] × 10^4 (M)	pHs
0.3	6.2	1.84	6.7
0.4	5.8	2.3	7.0
0.5	5.4	2.7	7.1
0.6	5.0	3.0	7.2
0.7	4.8	3.3	7.3
0.8	4.4	3.6	7.4
0.9	4.2	3.8	7.4
1.0	4.0	4.0	7.5

Table II. Final pH and Component Concentration of the Formulations Containing FLU and PK-Im

FLU/PK-Im	[PK-Im] × 10^4 (M)	[FLU] × 10^4 (M)	pHs
0.3	6.2	1.84	6.8
0.4	5.8	2.3	7.0
0.5	5.4	2.7	7.1
0.6	5.0	3.0	7.3
0.7	4.8	3.3	7.4
0.8	4.4	3.6	7.7

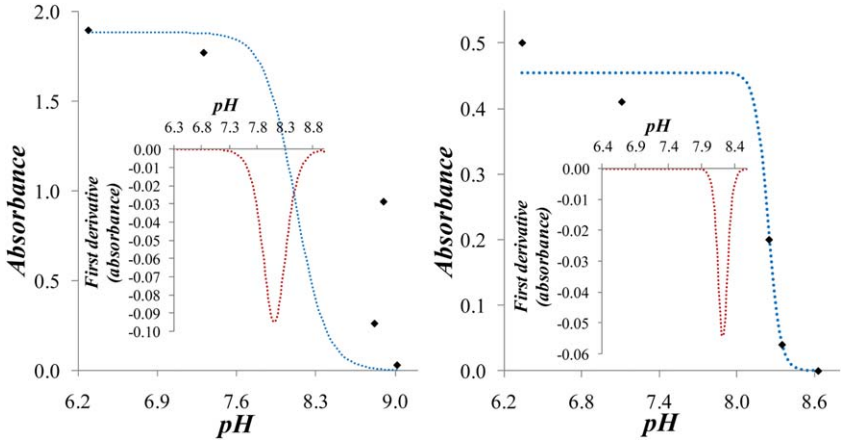

Figure 2. OA precipitation pH at 1×10^{-3} M (left) and 2×10^{-4} M (right). [Color figure can be viewed in the online issue, which is available at wileyonlinelibrary.com.]

dosage frequency, and protecting the encapsulated drug from undesired effects of external conditions.[32] All these advantages may have important implications in aquaculture as well as in human health therapies and environmental issues.

Current techniques to encapsulate hydrophilic drugs within polymeric micro- and nanostructures involve double emulsion methods,[33] layer-by-layer (LbL) assembly,[34,35] inclusion in polymer matrices such as polymer nanoaggregates, and in polymer micelles.[36] In most cases, these methods require the use of organic solvents[37–40] to dissolve low water-soluble components, which would further assemble upon solvent displacement and evaporation. Given that PK-Im may produce aromatic–aromatic interactions with aromatic counterions, and the need to generate nanoparticles containing antibiotics, the aim of this study is to explore the ability of PK-Im to bind and disperse OA and FLU in an out-of-equilibrium process where organic solvents are not used and in which, upon acid–base neutralization reaction, molecules change their hydrophilic/hydrophobic properties and rearrange in order to produce nanostructures. It will be shown that nanoprecipitates composed of this polymer and target antibiotics can be formed by controlling the mixture process, so that a final pH close to neutrality is achieved. Dynamic light scattering and UV-vis spectroscopy will be used to observe these processes.

EXPERIMENTAL

Reagents

Histamine (CAS 51-45-6) (Sigma-Aldrich), OA (CAS 14698-29-4) (Sigma-Aldrich), and FLU (CAS 42835-25-6) (Sigma-Aldrich) were commercially available and used as received. The respective structures are drawn in Figure 1.

Equipment

Distilled water was deionized by a Simplicity Millipore deionizer. The pH was controlled on an UltraBasic Denver Instrument pH meter. UV-vis measurements were performed in a Helios γ spectrophotometer. Size and zeta potential measurements were performed in a zetasizer Nano-ZS (Malvern Instruments) with backscatter detection (173°), controlled by the Dispersion Technology Software (DTS 6.2, Malvern).

Procedures

PK-Im Synthesis. The alternating aliphatic polyketone (PK50), precursor of PK-Im, was synthesized according to Mul, *et al.*[41] using carbon monoxide and both ethylene and propylene as

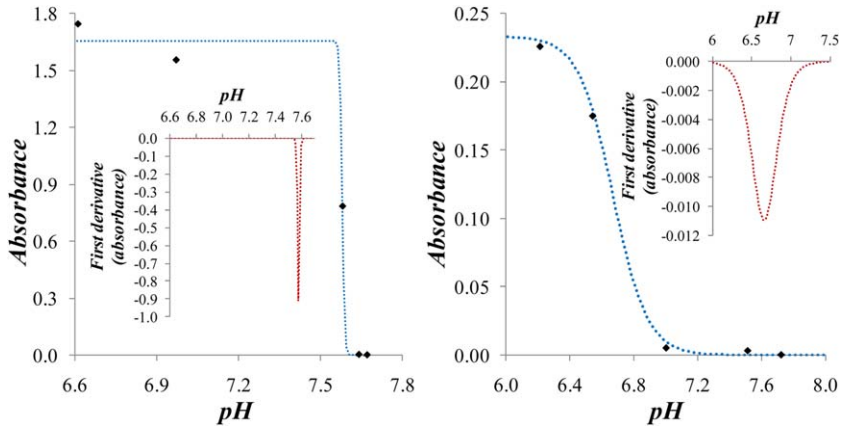

Figure 3. FLU precipitation pH at 1×10^{-3} M (left) and 2×10^{-4} M (right). [Color figure can be viewed in the online issue, which is available at wileyonlinelibrary.com.]

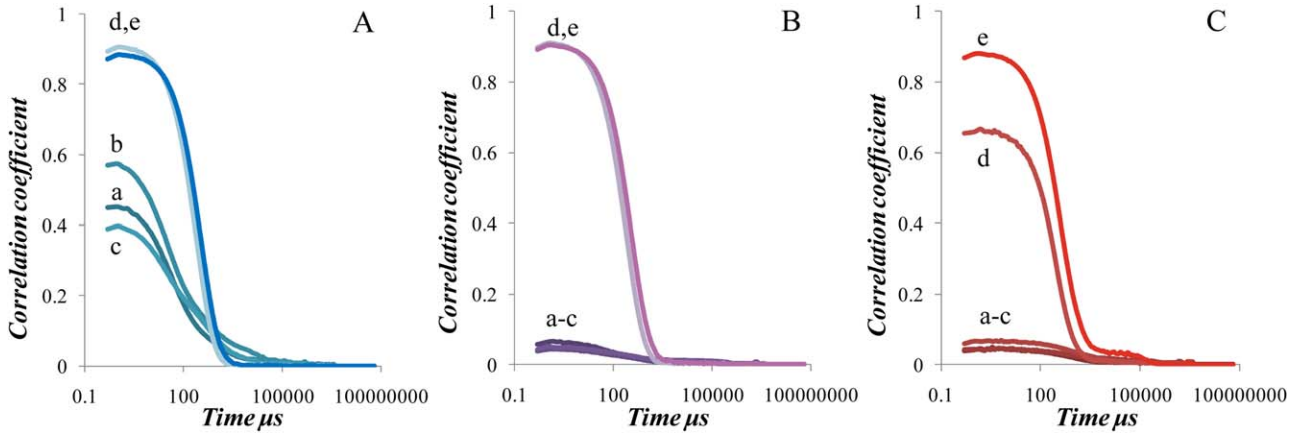

Figure 4. Correlograms obtained by DLS of PK-Im at concentrations of 1×10^{-3} (A), 1×10^{-4} (B), and 1×10^{-5} M (C), and pH values of 3 (a), 5 (b), 5.5 (c), 6 (d), and 7 (e). [Color figure can be viewed in the online issue, which is available at wileyonlinelibrary.com.]

hydrocarbons. The resulting terpolymer presents a total olefin content of 50% of ethylene and 50% of propylene (PK50, Mw 5350 Da). Its formula weight considering the diketone moieties was calculated to be 126 g/mol. The synthesis of PK-Im was carried out by means of the Paal-Knorr reaction of pK50 with histamine, according to the scheme shown in Figure 1. About 40 g of the polyketone PK50 were weighed into a glass reactor fitted with a mechanical stirrer and a reflux condenser. The reactor was heated to a temperature of 110°C and histamine was added dropwise during the first hour. Stoichiometric amounts of amine and dicarbonyl moieties have been used. The reaction was allowed to proceed for another 3 h. The reflux condenser was removed in the last hour to allow the produced water to evaporate. The obtained dark brown product was ground into small particles (freezing the material if necessary). The obtained particles were washed with Milli-Q water, and then freeze-dried for 24 h. The resulting polymer was characterized spectroscopically and by elemental analysis, presenting 1,4-dicarbonyl conversion of 71.1%, and a calculated formula weight per mole of ionizable amine groups of 266 g/mol. Details on the polymer characterization and formula weight calculation can be found elsewhere.[23]

Solubility Studies. Aqueous stock solutions of PK-Im, OA, and FLU were prepared at concentrations of 1×10^{-2}, 1×10^{-3}, and 1×10^{-3} M, respectively. In order to dissolve the reactants, the pH of the stock solutions was adjusted to 5.4, 10.5, and 11 for PK-Im, OA, and FLU, respectively. Then, the solubility of the pristine antibiotics as a function of the pH was searched by turbidimetry in a UV-vis spectrometer using quartz vessels with path lengths of 1 cm, and registering the signal at 400 nm, where OA and FLU do not absorb. The solubility test was conducted diluting the antibiotic stock solutions to 1×10^{-3}, 2×10^{-4}, and 1×10^{-5} M and successively lowering the pH with the aid of aqueous HCl. HCl solutions were prepared at different concentrations in order to use the minimum volume so that the final volume of the antibiotic solution does not change significantly. The obtained data were treated with the OriginPro 8 software, and non-linear fitting was done using the Boltzman sigmoidal function. The solubility of PK-Im was also studied. Solutions of the polymer were prepared at concentrations of 1×10^{-3}, 1×10^{-4}, and 1×10^{-5} M and pH 3. DLS responses (intensity distributions) where registered at 25°C for these solutions after successively adjusting the pH from 3 to 7. A laser beam operating at 633 nm was used and detection was done at a fixed angle of 173°. Each measurement was done in triplicate. A multimodal analysis was used for data treatment. Results were considered valid under the DTS 6.2 software criteria.

Nanoprecipitate Formation. Nanoprecipitates of PK-Im, PK-Im/OA, and PK-Im/FLU were obtained by adjusting physicochemical parameters of the corresponding stock solutions. The

Table III. Size, PDI Values, and Zeta Potential of PK-Im Aggregates at Different pHs at a PK-Im Concentration of 1×10^{-3} M

pH	Hydrodynamic diameter (nm)	PDI	Zeta potential (mV)
2.9	183	0.3	21
4.8	136	0.4	23
5.5	175	0.5	31
5.8	212	0.4	28
6.4	188	0.3	36
7.0	167	0.3	30
7.4	227	0.3	27

Table IV. Size, PDI Values, and Zeta Potential of PK-Im Aggregates at Different pHs at a PK-Im Concentration of 1×10^{-4} M

pH	Hydrodynamic diameter (nm)	PDI	Zeta potential (mV)
2.9	370	0.7	11
4.9	156	0.5	7.0
5.5	559	0.6	11
5.8	239	0.9	14
6.1	190	0.4	41
6.8	170	0.3	39
7.0	241	0.4	36

Table V. Size, PDI Values, and Zeta Potential of PK-Im Aggregates at Different pHs at a PK-Im Concentration of 1×10^{-5} M

pH	Hydrodynamic diameter (nm)	PDI	Zeta potential (mV)
3.0	336	0.7	5.2
5.2	549	0.6	2.4
5.4	5742	0.8	3.0
6.0	314	0.4	26
6.3	322	0.5	24
6.7	200	0.4	31
6.9	288	0.4	35

pH and concentration of the stock solutions allowed us to produce different mixtures whose final pH value was close to neutrality. The mixing protocol consisted on pouring dropwise under vigorous stirring an amount of the antibiotic solution into the polymer solution until the desired concentration was reached. The final concentration and pH values of the resulting mixtures are listed in Tables I and II. The mixtures were controlled by DLS as described above.

RESULTS AND DISCUSSION

Solubility of OA, FLU, and PK-Im

The solubility of OA and FLU in water was tested at three different concentrations (1×10^{-3}, 2×10^{-4}, and 1×10^{-5} M) as a function of the pH. The relative intensity of scattering at different pH values is plotted in Figures 2 and 3. Adjusting the data to fit a Boltzmann sigmoidal curve and further derivation allows finding the transition pH at which the antibiotics precipitate at the different concentrations, related to their acid–base equilibrium for which the carboxylic group is responsible (see Figure 1). It can be seen that OA needs more basic conditions to be dissolved than FLU. At a concentration of 1×10^{-3} M, OA is soluble from pH 9.0, and 8.6 at a concentration of 2×10^{-4} M. At a concentration of 1×10^{-5} M, OA was soluble at all the tested pH values. Results for FLU showed solubility at pH values higher than 7.6 at a concentration of 1×10^{-3} M, and higher than 7.0 at a concentration of 2×10^{-4} M, while at a concentration of 1×10^{-5} M FLU was soluble at all the tested pH values.

The solubility of PK-Im at three different concentrations was tracked by DLS in order to follow the collapse of the cationic polymer by increasing the pH and consequently deprotonating the imidazolium groups, which act as weak acids. The results can be seen in Figure 4 and Tables (III–V). At pH 3, the imidazolium groups are highly protonated, and the polymer is more hydrophilic. A low Tyndall effect was found for all the samples, revealed by a low intensity of scattering, which is lower at lower concentrations. Increasing the pH changes the DLS responses, as can be seen in Figure 4, where the corresponding correlograms are shown. Monomodal particle size distributions were found. The results show that at low pH such as pH 3, the polymer shows amphiphilic properties and undergoes self-aggregation. When the pH is increased, the imidazolium groups deprotonate, decreasing the repulsive electrostatic interaction between segments. Therefore, some parts of the polymeric chains become more hydrophobic and, as a result, the process of aggregation to form a hydrophobic core is enhanced. At pHs between 5.5 and 7.5, an intense Tyndall effect is observed (see Figure 4), and aggregates of hydrodynamic diameters ranging in the submicron size are formed, that present a positive zeta potential high enough to allow stability at pHs near neutrality (see Tables (III–V)). The corresponding correlograms show monoexponential decays. At pHs higher than 7.5, the deprotonation of the polymer induces its precipitation in the form of macroprecipitates.

PK-Im/OA and PK-Im/FLU Nanoparticles

Nanoprecipitates were obtained by mixing a 1×10^{-2} M PK-Im solution at pH 5.4 and 1×10^{-3} M OA or FLU solutions at pH 10.5 and 11, respectively. The final pH of the mixtures reached values near neutrality, as can be seen in Tables I and II. The final concentration of the reactants can be correlated to the results of solubility described above. Mixtures containing only the antibiotics OA and FLU at a concentration of 2×10^{-4} M precipitated as visible macroparticles at pHs under 8.6 and 7.0, respectively. On the other hand, in the presence of PK-Im, the mixtures containing the antibiotics at comparable or higher

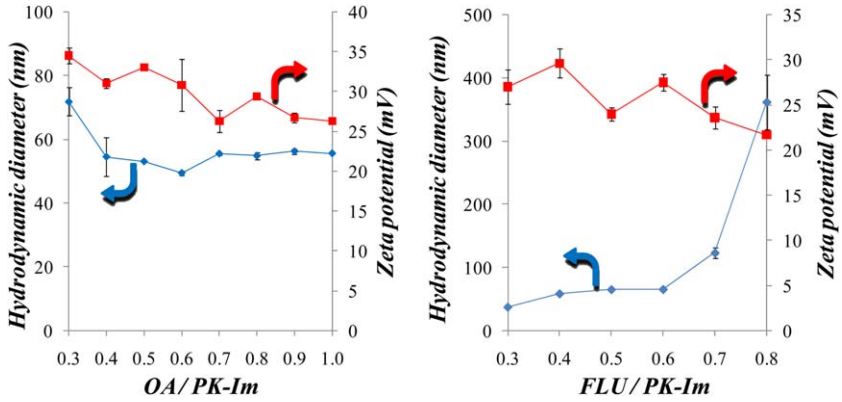

Figure 5. Size (◆) and (■) zeta potential of particles composed of OA and PK-Im (left) and FLU and PK-Im (right) as a function of their relative concentration. [Color figure can be viewed in the online issue, which is available at wileyonlinelibrary.com.]

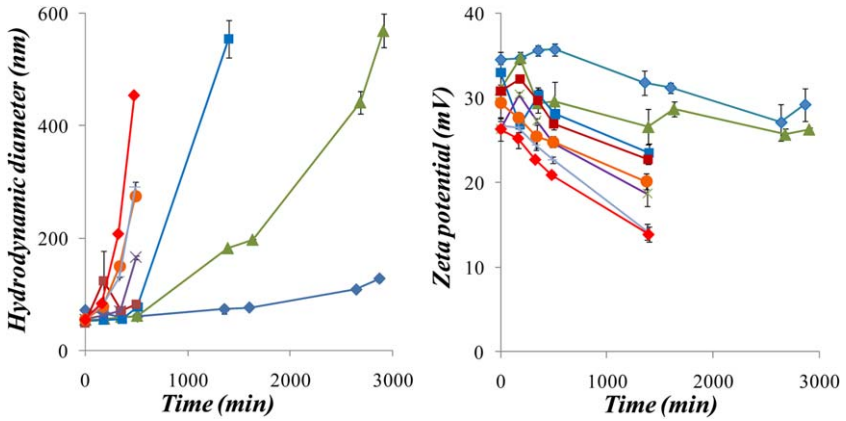

Figure 6. Size (left) and zeta potential (right) of OA/PK-Im nanoparticles as a function of time for OA/PK-Im molar ratios of 0.3 (◆), 0.4 (▲), 0.5 (■), 0.6 (■), 0.7 (×), 0.8 (•), 0.9 (+), and 1.0 (◆). [Color figure can be viewed in the online issue, which is available at wileyonlinelibrary.com.]

concentrations appeared as nanoprecipitates instead of macroprecipitates, when the pH of the mixtures ranged between 6.7 and 7.5, as can be seen in Figure 5, where results obtained by DLS are shown. DLS results showed monomodal intensity distributions. During the mixing process, the collapse of the polymer is accompanied by the co-precipitation of the antibiotic. The size of the precipitates takes values at the submicron scale, which indicates that the antibiotic is imbibed in the polymeric matrix.

The results concerning size and zeta potential of the nanoparticles have been plotted in Figure 5 as a function of the antibiotic/polymer ratio. For OA the resulting pH ranged between 6.7 and 7.5, and the respective particle size ranged between 49.4 and 71.8 nm, whilst the zeta potential ranged between 26.3 and 34.5 mV (Figure 5 left). The nanoparticles found present smaller hydrodynamic diameters than those corresponding to the pristine polymer, indicating a more compact configuration of the aggregates due to higher hydrophobicity at the core of the nanoparticles. The size of the nanoparticles decreases as the antibiotic/polymer ratio increases. The zeta potential, in contrast, decreases as the antibiotic/polymer ratio increases, which may produce instability of the nanoprecipitates. In order to observe this, stability of the nanoparticles was analyzed by observing the size and zeta potential evolution as a function of time. Figure 6 shows that stable nanoparticles are found under a high excess of the polymer, which ensures the presence of enough imidazolium functional groups at the particle surface (caused both by the higher excess of protonable groups and the lower pH reached) to stabilize the particle by charge repulsion, so that size and zeta potential changes in time are moderate.

For FLU, the pH ranged between 6.8 and 7.7, the particle size ranged between 37.9 and 361.7 nm, and the respective zeta potential ranged between 27.0 and 21.7 mV (Figure 5 right). It can be considered that the zeta potential is somehow low to guarantee the stability of the nanoparticles. In fact, at FLU/PK-Im ratios higher than 0.6, the sharp increase in nanoparticle size indicated higher aggregation of molecules resulting in bigger particles. Note that up to a FLU/PK-Im ratio of 0.6, and as in the case of OA, the particle size is significantly lower than that for corresponding concentrations of the pristine polymer, indicating a shrinking effect produced by the antibiotic. However, at FLU/PK-Im over 0.6, the pH obtained is high enough (higher than 7.3) to allow FLU to dissolve in water, due to its higher hydrophilicity, and the particle size of the precipitates

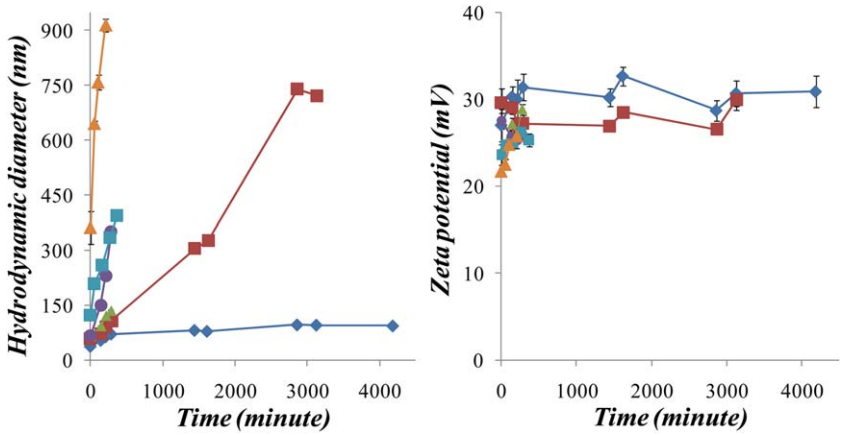

Figure 7. Size (left) and zeta potential (right) of FLU/PK-Im nanoparticles as a function of time for FLU/PK-Im molar ratios of 0.3 (◆), 0.4 (■), 0.5 (▲), 0.6 (•), 0.7 (■), and 0.8 (▲). [Color figure can be viewed in the online issue, which is available at wileyonlinelibrary.com.]

exponentially increases, possibly due to the collapse of the polymer alone. Stability analyses shown in Figure 7 reflect that the size of the precipitates keeps increasing over time for the samples richer in the antibiotic. Thus, stable submicron particles can be synthesized at an OA/PK-Im of 0.3, reaching a pH of 6.7, showing 72 nm of hydrodynamic radius (PDI 0.5), zeta potential of 35 mV. Similarly, at a FLU/PK-Im of 0.3, the pH was 6.8, and stable submicron particles were synthesized showing 40 nm of hydrodynamic radius (PDI 0.4), and zeta potential of 27 mV.

Precipitation upon mixing two solutions of different pH values is an out-of-equilibrium process. Kinetically, the slowest movements may be ascribed to conformational changes and translational movements of the polymer chains. The diffusion of the antibiotics is a faster process so that, in order the molecules can co-precipitate, the antibiotics should bind the polymer by means of both long-range electrostatic interactions and short-range secondary interactions, such as short-range electrostatic and aromatic–aromatic interactions, before nanoprecipitation is complete. Short-range electrostatic interactions may produce ion pairs that stabilize the respective charges of both imidazolium and antibiotic ions and render the ensemble hydrophobic characteristics. Thus, even if most of the imidazolium groups undergo deprotonation and consequently lose their charges, remaining imidazolium compounds may be bound to the remaining charged antibiotics. These ion pairs tend to self-aggregate and stabilize into hydrophobic domains produced by the main chain of the polymer as well as by the polymeric segments with imidazolium groups that have lost their charge. In addition, uncharged antibiotic molecules may remain confined in these hydrophobic domains. A positive zeta potential indicates the presence of charged imidazolium residues at the surface of the particles, which stabilize them preventing their aggregation. Successful formation of stable nanoparticles comprised of both PK-Im and the antibiotics depends on the relative concentration of both reactants, and an excess of the polymer provides higher stability. Thus, the hydrophobicity and the consequent collapse of the polymeric system is tuned by the relative amount of antibiotic in the formulation.

Final Remarks

Here we have shown a method to nanodisperse the antibiotics OA and FLU by the aid of an easy-to-obtain synthetic polymeric matrix derived from alternated polyketones and histamine. The method shown here for the nanodispersion of the antibiotics OA and FLU presents the advantage that no organic solvent is used. The nanoencapsulation of these antibiotics occurs at physiologic pH, so that the formulations can improve the antibiotic dispersability at physiological conditions. Nanoformulated OA and FLU antibiotics could be used in aquaculture and human health therapies, with potential advantages in dosage efficacy, formulation efficiency, and environmental security.

CONCLUSION

Our study shows that it is possible to nanodisperse the two antibiotics OA and FLU at neutral pH at which they are poorly water-soluble by the aid of a synthetic polyelectrolyte presenting aromatic, charged imidazolium pendant groups, derived from a polyketone. The process is conducted in water so that the use of organic solvents is avoided. The two antibiotics undergo macroprecipitation when lowering the pH under pH 7. On the other hand, the weak acid polyelectrolyte presenting imidazolium pendant groups is soluble in water at pHs lower than 5.5, showing amphiphilic properties. In the range of pH 5.5 to 7.5, progressive deprotonation of the polymer increases it hydrophobicity and the system collapses forming submicron particles. By mixing stock solutions of the antibiotic at basic pH and stock solutions of the polymer at acid pHs, acid–base reaction occurs. During this out-of-equilibrium process, interactions between the antibiotics and the polymer functional groups occur. The antibiotics and the polymer assemble, and submicron particles containing the antibiotics are formed. Apart from hydrophobic interactions, secondary interactions such as short-range electrostatic interactions and aromatic–aromatic interactions may stabilize the assemblies. An excess of the polymer is necessary in order to provide enough superficial charge to the particles to stabilize them. Thus, stable submicron particles at pH 6.7–6.8 can be synthesized at an antibiotic/PK-Im ratio of 0.3 showing a zeta potential of 35 mV and 72 nm of hydrodynamic radius for OA/PK-Im (PDI 0.5), and a zeta potential of 27 mV and 38 nm of hydrodynamic radius for FLU/PK-Im (PDI 0.4). The use of nanodispersed antibiotic formulations may be of advantage for animal and human treatment of diseases, minimizing environmental impacts.

ACKNOWLEDGMENTS

The authors thank Fondecyt (Grants No. 3110153 and 1120514, Chile), for financial support. Esteban Araya-Hermosilla thank the Programa de Capital Humano Avanzado (PFCHA) Conicyt, Becas Chile.

REFERENCES

1. Bütün, V.; Armes, S. P.; Billingham, N. C.; Tuzar, Z.; Rankin, A.; Eastoe, J.; Heenan, R. K. *Macromolecules* **2001**, *34*, 1503.
2. Báñez, M. V.; Robinson, K. L.; Vamvakaki, M.; Lascelles, S. F.; Armes, S. P. *Polymer* **2000**, *41*, 8501.
3. Jones, M. C.; Ranger, M.; Leroux, J. C. *Bioconjugate Chem.* **2003**, *14*, 774.
4. Hong, H.; Mai, Y.; Zhou, Y.; Yan, D.; Cui, J. *Macromol. Rapid Comm.* **2007**, *28*, 591.
5. Schild, H. G. *Progr. Polymer Sci.* **1992**, *17*, 163.
6. Sanz, E.; Valeriani, C.; Vissers, T.; Fortini, A.; Leunissen, M. E.; van Blaaderen, A.; Frenkel, D.; Marjolein, D. *J. Phys. Condens. Matter* **2008**, *20*, 494247.
7. Bochicchio, D.; Videcoq, A.; Ferrando, R. *Phys. Rev. E* **2013**, *87*, 022304.
8. Zhang, R.; Jha, P. K.; Olvera de la Cruz, M. *Soft Matter* **2013**, *9*, 5042.
9. Mortimer, D. A. *Polymer Int.* **1991**, *25*, 29.
10. Kumar, A.; Srivastava, A.; Galaev, I. Y.; Mattiasson, B. *Progr. Polymer Sci.* **2007**, *32*, 1205.

11. Qiu, Y.; Park, K. *Adv. Drug Deliv. Rev.* **2001**, *31*, 321.
12. Lee, H.; Boyce, J. R.; Nese, A.; Sheiko, S. S.; Matyjaszewski, K. *Polymer* **2008**, *49*, 5490.
13. Penga, S.; Bhushan, B. *RSC Adv.* **2012**, *2*, 8557.
14. Dai, S.; Ravi, P.; Tam, K. C. *Soft Matter* **2008**, *4*, 435.
15. Laguecir, A.; Ulrich, S.; Labille, J.; Fatin-Rouge, N.; Stoll, S.; Buffle, J. *Eur. Polym. J.* **2006**, *42*, 1135.
16. Mauser, T.; Déjugnat, C.; Sukhorukov, G. B. *J. Phys. Chem. B* **2006**, *110*, 20246.
17. Barba, A.; Dalmoro, A.; De Santis, F.; Lamberti, G. *Polym. Bull.* **2009**, *62*, 679.
18. Rivas, B. L.; Sánchez, J.; Pooley, S. A.; Basaez, L.; Pereira, E.; Bucher, C.; Royal, G.; Aman, E. S.; Moutet, J. C. *Macromol. Symp.* **2010**, *296*, 416.
19. Moreno-Villoslada, I.; González, F.; Arias, F.; Villatoro, J. M.; Ugarte, R.; Hess, S.; Nishide, H. *Dyes Pigments* **2009**, *82*, 401.
20. Moreno-Villoslada, I.; Torres-Gallegos, C.; Araya-Hermosilla, R.; Nishide, H. *J. Phys. Chem. B* **2010**, *114*, 4151.
21. Gómez-Tardajos, M.; Pino-Pinto, J. P.; Díaz-Soto, C.; Flores, M. E.; Gallardo, A.; Elvira, C.; Reinecke, H.; Nishide, H.; Moreno-Villoslada, I. *Dyes Pigments* **2013**, *99*, 759.
22. Ruthard, C.; Maskos, M.; Yildiz, H.; Gröhn, F. *Macromol. Rapid Comm.* **2011**, *32*, 523.
23. Toncelli, C.; Pino-Pinto, J. P.; Sano, N.; Picchioni, F.; Broekhuis, A. A.; Nishide, H.; Moreno-Villoslada, I. *Dyes Pigments* **2013**, *98*, 51.
24. Gröhn, F. *Soft Matter* **2010**, *6*, 4296.
25. Ruthard, C.; Maskos, M.; Yildiz, H.; Gröhn, F. *Macromol. Chem. Phys.* **2009**, *210*, 1678.
26. Cong, Y.; Gunari, N.; Zhang, B.; Janshoff, A.; Schmidt, M. *Langmuir* **2009**, *25*, 6392.
27. Araya-Hermosilla, R.; Broekhuis, A. A.; Picchioni, F. *Eur. Polym. J.* **2014**, *50*, 127.
28. Zhang, Y.; Broekhuis, A. A.; Stuart, M. C. A.; Picchioni, F. *J. Appl. Polym. Sci.* **2008**, *107*, 262.
29. Samuelsen, B.; Lunestad, B. *Dis. Aquat. Org.* **1996**, *27*, 13.
30. Lai, H. T.; Lin, J. J. *Chemosphere* **2009**, *75*, 462.
31. Myhr, A. I.; Myskja, B. K. *Nanoethics* **2011**, *5*, 73.
32. Zhang, L.; Gu, F.; Chan, J.; Wang, A.; Langer, R.; Farokhzad, O. *Clin. Pharmacol. Therapeut.* **2008**, *83*, 761.
33. Cohen-Sela, E.; Chorny, M.; Koroukhov, N.; Danenberg, H. D.; Golomb, G. *J. Contr. Release* **2009**, *133*, 90.
34. Mora-Huertas, C. E.; Fessi, H.; Elaissari, A. *Int. J. Pharmaceut.* **2010**, *385*, 113.
35. Yan, S.; Zhu, J.; Wang, Z.; Yin, J.; Zheng, Y.; Chen, X. *Eur. J. Pharm. Biopharm.* **2011**, *78*, 336.
36. Barba, A.; Dalmoro, A.; d'Amore, M.; Vascello, C.; Lamberti, G. *J. Mater. Sci.* **2014**, *49*, 5160.
37. Francis, M. F.; Cristea, M.; Winnik, F. M. *Pure Appl. Chem.* **2004**, *76*, 1321.
38. Yokoyama, M.; Fukushima, S.; Uehara, R.; Okamoto, K.; Kataoka, K.; Sakurai, Y.; Okano, T. *J. Contr. Release* **1998**, *50*, 79.
39. Fournier, E.; Dufresne, M.; Smith, D.; Ranger, M.; Leroux, J. *Pharmaceut. Res.* **2004**, *21*, 962.
40. Kwon, G.; Naito, M.; Yokoyama, M.; Okano, T.; Sakurai, Y.; Kataoka, K. *J. Contr. Release* **1997**, *48*, 195.
41. Mul, W. P.; Dirkzwager, H.; Broekhuis, A. A.; Heeres, H. J.; van der Linden, A. J.; Guy Orpen, A. *Inorg. Chim. Acta* **2002**, *327*, 147.